Pergamon

Int. J. Solids Structures Vol. 32, No. 23, pp. 3377–3392, 1995

0020–7683/95 $9.50 + .00

0020–7683(94)00311–4

EFFECTS OF INITIAL CURVATURE ON THE DYNAMIC STABILITY OF A BEAM WITH TIP MASS SUBJECTED TO AXIAL PULSATING LOADS

H. P. LEE
Department of Mechanical and Production Engineering, National University of Singapore, 10 Kent Ridge Crescent, Singapore 0511

(*Received* 2 *March* 1994; *in revised form* 20 *November* 1994)

Abstract—The linearized equation of motion in matrix form of an Euler–Bernoulli inextensible beam with initial curvature and a tip mass subjected to axial pulsating loads is formulated based on Lagrangian approach and the assumed mode method. The effect of initial curvature is shown to be contained in the kinetic energy of the tip mass as well as the work done by the axial loads. Using Bolotin's method, the linearized equation of motion is converted to the standard form of an eigenvalue problem for computing the principal instability regions. The initial curvature of the beam is found to have no effect on the dynamic stability of the beam if there is no tip mass. The effects of various prescribed initial shapes of the beam, the tip mass, the frequency and magnitude of load perturbation on the stability behaviors are investigated for a simply supported beam.

INTRODUCTION

A slender beam with slight initial curvature subjected to tensile pulsating loads has been shown by Carlson *et al.* (1980) to exhibit large principal regions of instability that resulted in unacceptably large amplitudes of vibration. In their work, a simply supported inextensible beam with a lumped mass and an axial spring at one end of the beam was analysed using Euler beam theory. Terms involving the effect of initial curvature were contained in the kinetic energy of the lumped mass, the potential energy of the spring as well as the work done by the tensile load. Other related studies on the vibration of a beam with initial slight curvature were reported by Yamaki and Mori (1980) and Yamaki *et al.* (1980) for the effect of periodic loading on a beam with initial axial displacement and initial deflection, Plaut and Johnson (1981) for the effect of initial thrust on the vibration of a shallow, sinusoidal arch pinned at both ends, and Johnson (1982) for the effect of initial thrust on the vibration of a shallow clamped circular arch. The relation between the induced axial force and the initial curvature of an extensible beam subjected to prescribed axial end displacement was reported by Dickinson (1980). The natural frequencies of simply supported and clamped beams with initial curvature were subsequently presented by Kim and Dickinson (1986) using Galerkin's method. Ilanko (1990) analysed the effect of partial axial end restraints and sliding end masses on the natural frequencies of an initially curved simply supported beam. The partial axial end restraints were enforced by two axial springs at the two ends. The beam was also assumed to be extensible. Saito and Koizumi (1982) investigated the steady state response of a simply supported inextensible beam carrying a concentrated mass at one end and subjected to a periodic axial displacement excitation at the other end under the influence of gravity. Although the effect of "axial inertia" of the beam, which was neglected in all the other reported studies, was included, the other more important effect of "geometric stiffness" due to the axial shortening of the beam and the presence of axial forces was not taken into consideration. The axial shortening due to the transverse bending of the beam could be significant for a beam with initial curvature. The induced axial forces on the beam could also be large for a beam with a heavy lumped mass subjected to high frequency of excitation.

In these studies, the initial shape of the beam was always assumed to be in the form of the first flexural mode for a simply supported beam, or was described by a combination of simple sine and cosine functions approximating the first flexural mode for a clamped beam.

Moreover, only the first unstable regions were provided in the stability studies. In this paper, the linearized equation of motion in matrix form of an Euler–Bernoulli inextensible beam with slight initial curvature subjected to pulsating axial loads is derived based on Lagrangian approach and the assumed mode method. A lumped mass is also assumed to be attached to one end of the beam. The linearized equation of motion is then converted to the standard form of an eigenvalue problem using Bolotin's method for computing the principal instability regions of the beam. The effects of various prescribed initial shapes of the beam and the tip mass on the instability regions are examined in the present study.

THEORY AND FORMULATIONS

A simple model of a uniform inextensible beam of length L subjected to axial tensile loads P is shown in Fig. 1. The term "inextensible" is commonly used [for example, Carlson *et al.* (1980)] to describe a beam with the axial displacement of the beam caused solely by its bending deflection. In other words, the potential energy of the beam consists only of the bending strain energy and the potential energy caused by the "geometric stiffness" of the beam due to the axial shortening and the presence of the axial forces. The remaining elastic strain energy of the beam due to the axial elastic deformation is neglected. The reasons for making this simplifying assumption will be presented in the following section. A lumped mass of mass M is attached to one end of the beam. The beam can be used as a simple model for the slider in a slider-crank mechanism. A set of right-handed mutually perpendicular unit vectors, $\mathbf{n}_1$, $\mathbf{n}_2$ and $\mathbf{n}_3$, is assumed to be fixed in the undeformed beam, with the $\mathbf{n}_1$ vector parallel to a line passing through the two ends of the beam. The initial shape of the beam is described by $y_0(x)$. The deformed shape of the beam at any instant is denoted by $y(x, t)$. The initial curvature and subsequent deflections of the beam are assumed to be small for the behavior of the beam to be described by the Euler–Bernoulli beam theory rather than resorting to more elaborate curved beam theories usually used for analysing arches and arc structures. Moreover, $y-y_0$ is assumed to be very much smaller than y_0 [see Ilanko (1990)]. The deformation of the beam is assumed to be confined to the plane defined by $\mathbf{n}_1$ and $\mathbf{n}_2$.

The elastic strain energy of the beam due to bending is

$$V_e = \tfrac{1}{2}EI\int_0^L \left(\frac{\partial^2 w}{\partial x^2}\right)^2 \mathrm{d}x, \tag{1}$$

where E and I are the Young's modulus and the central principal second moment of area of the cross-section of the beam. The variable w is defined as

$$w = y-y_0. \tag{2}$$

To compute the kinetic energy of the tip mass M, one must first obtain an expression for the axial displacement at the tip mass given by

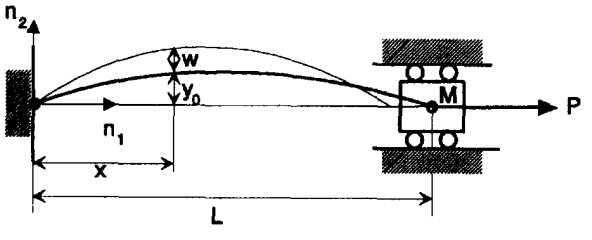

Fig. 1. A beam with a prescribed initial curvature and a tip mass subjected to pulsating axial tensile load.

$$u_L = \frac{1}{2}\int_0^L \left(\left(\frac{\partial w}{\partial x}\right)^2 + 2\frac{\partial y_0}{\partial x}\frac{\partial w}{\partial x}\right)\mathrm{d}x. \tag{3}$$

If the beam is not assumed to be inextensible, the above expression needs to be replaced by

$$u_L = \frac{1}{2}\int_0^L \left(\left(\frac{\partial w}{\partial x}\right)^2 + 2\frac{\partial y_0}{\partial x}\frac{\partial w}{\partial x}\right)\mathrm{d}x - \frac{(P - M\ddot{u}_L)L}{EA}. \tag{4}$$

The last term is caused by the axial elastic deformation of the beam due to the axial force $(P - M\ddot{u}_L)$ applied at the right end of the beam. The presence of such a term will complicate the computation of u_L unless there is no lumped mass. In the following derivation, the axial rigidity EA is assumed to be large for the axial displacement due to the axial elastic deformation of the beam. Such a beam is termed inextensible.

The derivation of eqn (3) can be found in the works by Carlson *et al.* (1980) and Ilanko (1990). A positive u_L is defined to be in the opposite direction of the tensile load P. Performing the time differentiation, $\dot{u}_L$ is given by

$$\dot{u}_L = \int_0^L \left(\frac{\partial w}{\partial x}\frac{\partial^2 w}{\partial x\,\partial t} + \frac{\partial y_0}{\partial x}\frac{\partial^2 w}{\partial x\,\partial t}\right)\mathrm{d}x. \tag{5}$$

The total kinetic energy T of the beam is

$$T = \tfrac{1}{2}m\int_0^L \dot{w}^2\,\mathrm{d}x + \tfrac{1}{2}M\dot{u}_L^2, \tag{6}$$

where m is the mass of the beam per unit length. The variable $\dot{w}$ is defined by $\mathrm{d}w/\mathrm{d}t$.

Using the assumed mode method, the quantity w can be expressed as

$$w = \sum_{i=1}^{n} q_i(t)\phi_i(x), \tag{7}$$

where ϕ_i are spatial functions that satisfy the prescribed geometric boundary conditions for the two ends of the beam. Similarly, the quantity y_0 can be expressed as

$$y_0 = \sum_{i=1}^{n} q_{0_i}\phi_i(x). \tag{8}$$

From the assumed functions for w and y_0 and assuming that $y_0 \gg w$, the term $\dot{u}_L$ in T can be expressed in matrix form as

$$\dot{u}_L^2 = \dot{\mathbf{q}}^{\mathrm{T}}\mathbf{Q}\mathbf{q}_0\mathbf{q}_0^{\mathrm{T}}\mathbf{Q}\dot{\mathbf{q}} + \text{higher order terms}, \tag{9}$$

where $\mathbf{Q}$ is defined as

$$(\mathbf{Q})_{ij} = \int_0^L \frac{\mathrm{d}\phi_i}{\mathrm{d}x}\frac{\mathrm{d}\phi_j}{\mathrm{d}x}\mathrm{d}x. \tag{10}$$

Neglecting the higher order terms and dropping all the other terms that do not involve $\mathbf{q}$ and $\dot{\mathbf{q}}$, the kinetic energy T and strain energy V_ε for a beam with a slight initial curvature can be expressed in matrix form as

$$T = \tfrac{1}{2}m\dot{\mathbf{q}}^{\mathrm{T}}\mathbf{M}\dot{\mathbf{q}} + \tfrac{1}{2}M\dot{\mathbf{q}}^{\mathrm{T}}\mathbf{S}\dot{\mathbf{q}} \tag{11}$$

$$V_e = \tfrac{1}{2}EI\mathbf{q}^{\mathrm{T}}\mathbf{K}\mathbf{q}. \tag{12}$$

The matrix $\mathbf{S} = \mathbf{Q}\mathbf{q}_0\mathbf{q}_0{}^{\mathrm{T}}\mathbf{Q}$. The matrices $\mathbf{M}$ and $\mathbf{K}$ are symmetric matrices defined as

$$(\mathbf{M})_{ij} = \int_0^L \phi_i\phi_j \,\mathrm{d}x \tag{13}$$

$$(\mathbf{K})_{ij} = \int_0^L \phi_i''\phi_j'' \,\mathrm{d}x. \tag{14}$$

The functions ϕ_i' and ϕ_i'' denote the first and second derivatives of ϕ_i with respect to x. The vectors $\mathbf{q}$, $\mathbf{q}_0$ and $\dot{\mathbf{q}}$ are $n \times 1$ column vectors.

The resulting Euler–Lagrange equation in matrix form is given by

$$\frac{\mathrm{d}}{\mathrm{d}t}\left(\frac{\partial T}{\partial \dot{\mathbf{q}}}\right) - \frac{\partial (T - V_e)}{\partial \mathbf{q}} = \mathbf{f}. \tag{15}$$

To obtain the generalized force vector $\mathbf{f}$. one must first express the axial displacement u_L in matrix form as

$$u_L = \tfrac{1}{2}\mathbf{q}^{\mathrm{T}}\mathbf{Q}\mathbf{q} + \mathbf{q}^{\mathrm{T}}\mathbf{Q}\mathbf{q}_0. \tag{16}$$

The virtual work δW of the axial tensile load P due to a virtual $\delta\mathbf{q}$ is given by

$$\delta W = -P(\delta\mathbf{q}^{\mathrm{T}}\mathbf{Q}\mathbf{q} + \delta\mathbf{q}^{\mathrm{T}}\mathbf{Q}\mathbf{q}_0). \tag{17}$$

There is a negative sign for P because a positive tensile load P is defined to be in the opposite direction of the positive axial displacement u_L due to the transverse deflection of the beam. The generalized force vector $\mathbf{f}$ can be computed from

$$\begin{aligned}\mathbf{f} &= \frac{\partial W}{\partial \mathbf{q}} \\ &= -P\mathbf{Q}\mathbf{q} - P\mathbf{Q}\mathbf{q}_0.\end{aligned} \tag{18}$$

The resulting linearized equation of motion is

$$(m\mathbf{M} + M\mathbf{S})\ddot{\mathbf{q}} + (EI\mathbf{K} + P\mathbf{Q})\mathbf{q} = -P\mathbf{Q}\mathbf{q}_0. \tag{19}$$

For simplicity, the following dimensionless quantities are introduced:

$$\tau = t\sqrt{\frac{EI}{mL^4}}, \quad \xi = \frac{x}{L}, \quad \sigma = \frac{PL^2}{EI}, \quad \kappa = \frac{M}{mL}. \tag{20}$$

The dimensionless w and y_0 are given by

$$\bar{w} = \frac{w}{L} = \sum_{i=1}^{n} \bar{q}_i(\tau)\phi_i(\xi) \tag{21}$$

$$\bar{r}_0 = \frac{r_0}{L} = \sum_{i=1}^{n} \bar{q}_{0_i}(\tau)\phi_i(\xi). \tag{22}$$

The resulting dimensionless equation of motion is

$$(\bar{\mathbf{M}} + \kappa\bar{\mathbf{S}})\ddot{\bar{\mathbf{q}}} + (\bar{\mathbf{K}} + \sigma\bar{\mathbf{Q}})\bar{\mathbf{q}} = -\sigma\bar{\mathbf{Q}}\bar{\mathbf{q}}_0. \tag{23}$$

The matrices in the above equation are defined as

$$(\bar{\mathbf{M}})_{ij} = \int_0^1 \phi_i\phi_j \, \mathrm{d}\xi \tag{24}$$

$$(\bar{\mathbf{K}})_{ij} = \int_0^1 \phi_i''\phi_j'' \mathrm{d}\xi \tag{25}$$

$$(\bar{\mathbf{Q}})_{ij} = \int_0^1 \phi_i'\phi_j' \, \mathrm{d}\xi. \tag{26}$$

The symmetric matrix $\bar{\mathbf{S}}$ is equal to $\bar{\mathbf{Q}}\bar{\mathbf{q}}_0\bar{\mathbf{q}}_0^{\dagger}\bar{\mathbf{Q}}$.

As an example, the dimensionless natural frequencies of a simply supported beam with various prescribed initial shapes and mass ratio κ are to be presented. For a beam simply supported at both ends, the assumed functions are

$$\phi_i(\xi) = \sqrt{2}\sin i\pi\xi. \tag{27}$$

The factor of $\sqrt{2}$ is to normalize the assumed functions. The matrix $\bar{\mathbf{M}}$ is equal to the identity matrix due to the orthogonality of the assumed functions. The matrix $\bar{\mathbf{K}}$ is a diagonal matrix with diagonal elements equal to $(i\pi)^4$ for $i = 1, \ldots, n$. The matrix $\bar{\mathbf{Q}}$ is also a diagonal matrix with diagonal elements equal to $(i\pi)^2$ for $i = 1, \ldots, n$. The other matrices can be computed using numerical integrations.

STABILITY ANALYSIS

The dimensionless tensile axial load σ is assumed to be of the form

$$\sigma = \sigma_0 + \sigma_s \sin\bar{\omega}\tau, \tag{28}$$

where σ_0 is the average dimensionless tensile axial load, σ_s and $\bar{\omega}$ are the dimensionless amplitude and frequency of the dimensionless sinusoidal load perturbation.

The stability analysis can be done by converting the homogeneous part of eqn (23) with the above prescribed sinusoidal function for the variation in axial load in the form of a second order differential equation with periodic coefficients of Mathieu–Hill type [see Masurekar and Gupta (1987); Takahashi (1981)]:

$$(\bar{\mathbf{M}} + \kappa\bar{\mathbf{S}})\ddot{\bar{\mathbf{q}}} + (\bar{\mathbf{K}} + \sigma_0\bar{\mathbf{Q}} + \sigma_s \sin\bar{\omega}\tau\bar{\mathbf{Q}})\bar{\mathbf{q}} = 0. \tag{29}$$

Using the method presented in Bolotin (1964), with additional references to subsequent application of this method by Carlson *et al.* (1980) and Takahashi (1981), the principal regions of instability of period $2T$ with $T = 2\pi/\bar{\omega}$ can be sought with $\bar{\mathbf{q}}$ in the form

$$\bar{\mathbf{q}} = \mathbf{c}\sin\frac{\bar{\omega}\tau}{2} + \mathbf{d}\cos\frac{\bar{\omega}\tau}{2}, \tag{30}$$

where $\mathbf{c}$ and $\mathbf{d}$ are arbitrary vectors.

Substituting eqn (30) into eqn (29) and equating the coefficients of the $\sin(\bar{\omega}\tau/2)$ and $\cos(\bar{\omega}\tau/2)$ terms, a set of linear homogeneous algebraic equations in terms of $\mathbf{c}$ and $\mathbf{d}$ can be obtained. The condition for non-trivial solutions is

$$\det\begin{vmatrix} -\frac{1}{4}\bar{\omega}^2(\bar{\mathbf{M}}+\kappa\bar{\mathbf{S}})+\bar{\mathbf{K}}+\sigma_0\bar{\mathbf{Q}} & \frac{1}{2}\sigma_s\bar{\mathbf{Q}} \\ \frac{1}{2}\sigma_s\bar{\mathbf{Q}} & -\frac{1}{4}\bar{\omega}^2(\bar{\mathbf{M}}+\kappa\bar{\mathbf{S}})+\bar{\mathbf{K}}+\sigma_0\bar{\mathbf{Q}} \end{vmatrix} = 0. \tag{31}$$

Instead of solving the above non-linear geometric equations for $\bar{\omega}$, the equation can be rearranged in the standard form of a generalized eigenvalue problem

$$\det\left|\begin{pmatrix} \bar{\mathbf{K}}+\sigma_0\bar{\mathbf{Q}} & \frac{1}{2}\sigma_s\bar{\mathbf{Q}} \\ \frac{1}{2}\sigma_s\bar{\mathbf{Q}} & \bar{\mathbf{K}}+\sigma_0\bar{\mathbf{Q}} \end{pmatrix} - \bar{\omega}^2\begin{pmatrix} \frac{1}{4}(\bar{\mathbf{M}}+\kappa\bar{\mathbf{S}}) & \mathbf{0} \\ \mathbf{0} & \frac{1}{4}(\bar{\mathbf{M}}+\kappa\bar{\mathbf{S}}) \end{pmatrix}\right| = 0. \tag{32}$$

The generalized eigenvalues $\bar{\omega}^2$ of the above generalized eigenvalue problem can be computed easily by any commercially available eigenvalue package.

There is a possibility that the initial shape $\bar{y}_0$ of the beam cannot be described by a combination of the assumed modes for $\bar{w}$. For example, the initial shape could resemble the first mode of the free vibration of a clamped–clamped beam. Such a shape function could not be one of the assumed mode for $\bar{w}$ as it violates the geometric boundary condition for the flexural vibration of the beam. For these cases,

$$\bar{y}_0 = \sum_{i=1}^{n} \bar{q}_{0_i}(\tau)\psi_i(\xi). \tag{33}$$

The matrix $\bar{\mathbf{S}}$ in eqn (29) needs to be modified as

$$\bar{\mathbf{S}} = \bar{\mathbf{R}}\bar{\mathbf{q}}_0\bar{\mathbf{q}}_0^{\mathrm{T}}\bar{\mathbf{R}}^{\mathrm{T}}, \tag{34}$$

with $\bar{\mathbf{R}}$ defined by

$$(\bar{\mathbf{R}})_{ij} = \int_0^1 \psi_i'\phi_j'\,\mathrm{d}\xi. \tag{35}$$

NUMERICAL RESULTS AND DISCUSSION

The principal dynamic instability regions with period $2T$ for an inextensible beam under tensile axial load perturbation with $\sigma_0 = 4$ and $\kappa = 0$, 1, 10 and 100 are presented in Fig. 2 using a 10-term approximation ($n = 10$) for w. This 10-term approximation function has been found to give numerical results that have converged for the first three unstable regions which are presented in the figure. Each of the unstable regions is bounded by two curves originating from a common point on the $\bar{\omega}$ axis with $\sigma_s = 0$. The initial shape of the beam is assumed to be the first assumed mode. As reflected in eqn (32), the unstable regions are not affected by variations in the initial curvature (which is contained in matrix $\bar{\mathbf{S}}$) when there is no tip mass (i.e. $\kappa = 0$). When the tip mass is increased, the first unstable region begins to be shifted to the left with smaller frequency of perturbation. The shifting of the first unstable region becomes more pronounced when the tip mass is large. An interesting phenomenon is that the remaining unstable regions remain relatively unaffected by variations in both the tip mass and the initial curvature.

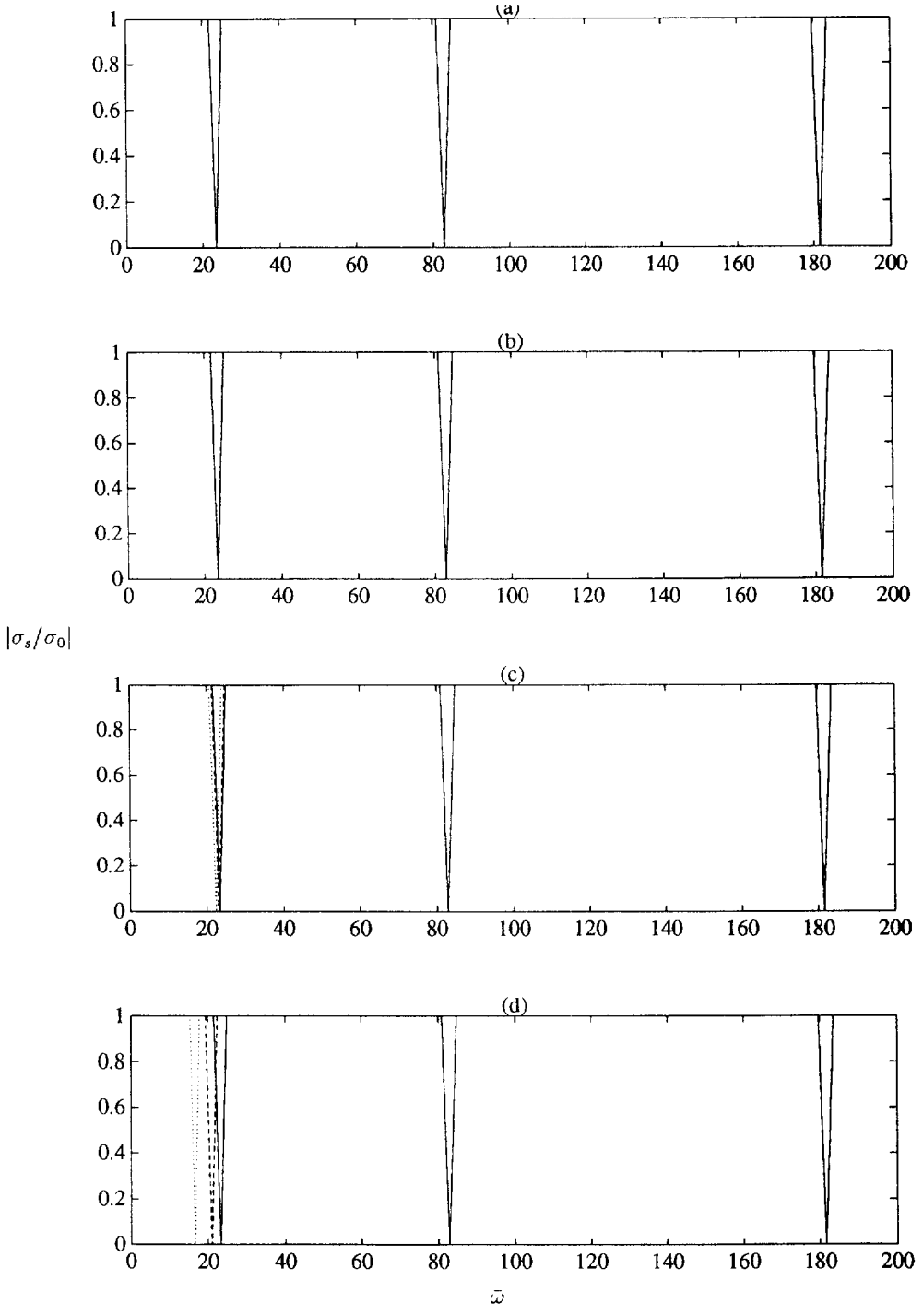

Fig. 2. The instability diagrams for an inextensible beam subjected to tensile pulsating axial loads. The initial shape is the first assumed mode. ———, $\bar{q}_{01} = 0.001$; - - - -, $\bar{q}_{01} = 0.005$; · · · · ·, $\bar{q}_{01} = 0.01$. (a) $\kappa = 0$, (b) $\kappa = 1$, (c) $\kappa = 10$, (d) $\kappa = 100$.

The effects of the initial prescribed shape of the beam on the instability regions are examined by specifying the initial shape to be the second and the third assumed modes. The average tensile axial load σ_0 is still kept to be 4. Numerical results are shown respectively in Figs 3 and 4. As expected, when there is no tip mass, the unstable regions are not affected by changes in the amplitude of the initial shape. When the initial shape is described by the second assumed mode of the beam, there is a large shift in the location of the second unstable region for $\kappa > 1$ (shown in Fig. 3), compared with the shifting of the first unstable

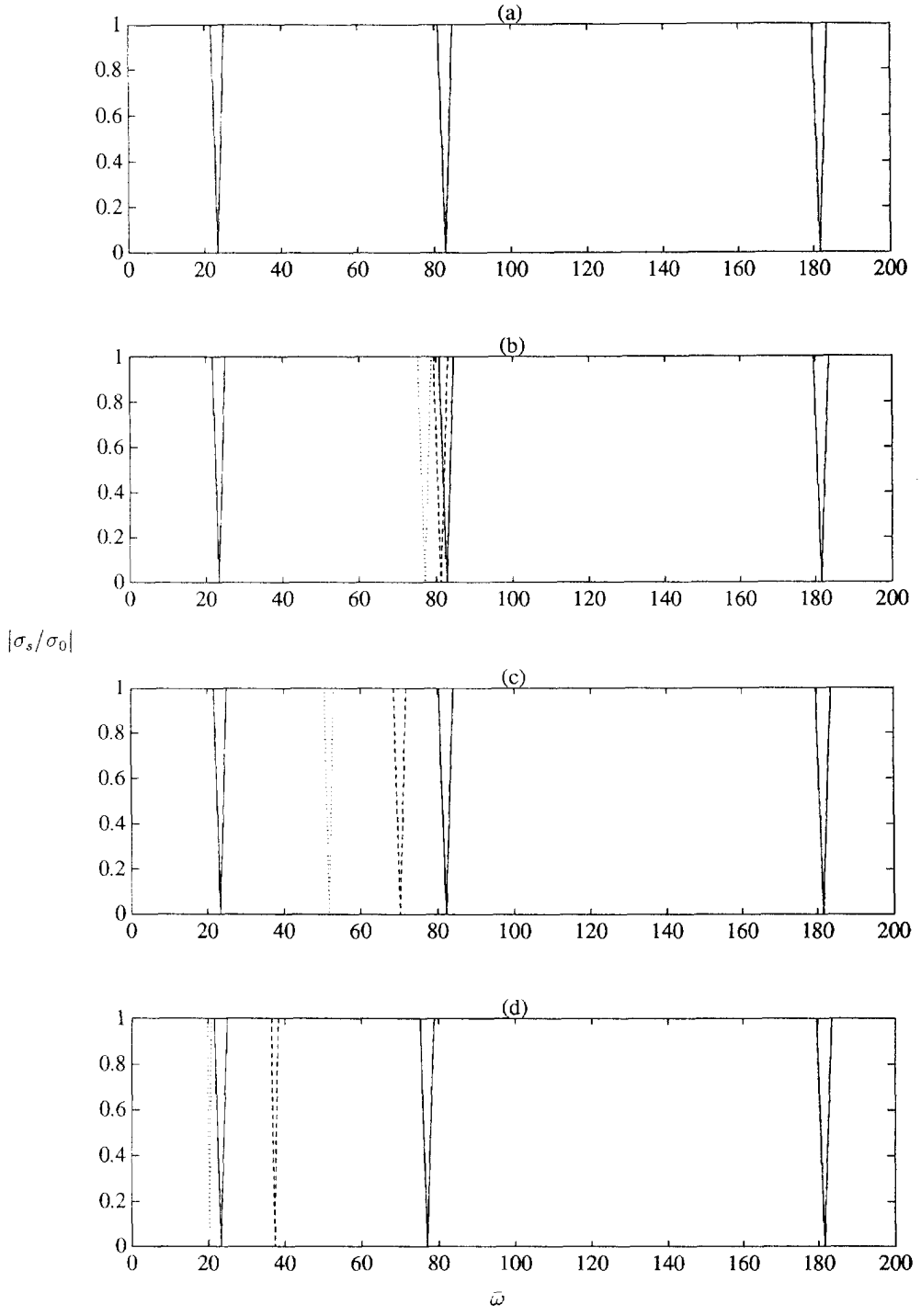

Fig. 3. The instability diagrams for an inextensible beam subjected to tensile pulsating axial loads. The initial shape is the second assumed mode. ——, $\bar{q}_{02} = 0.001$; - - - -, $\bar{q}_{02} = 0.005$; · · · · ·, $\bar{q}_{02} = 0.01$. (a) $\kappa = 0$, (b) $\kappa = 1$, (c) $\kappa = 10$, (d) $\kappa = 100$.

region with the initial shape described by the first assumed mode (shown in Fig. 2). The shifting becomes more pronounced when the tip mass is large. The larger shifting in the unstable region is due in part to the larger prescribed initial curvature of the beam, as a beam in the second assumed mode with a prescribed value of $\bar{q}_{02}$ has a larger curvature than a beam in the first assumed mode with the same prescribed value of $\bar{q}_{01}$. However, the curvature of the beam is still kept to be small ($\bar{q}_{02} \leqslant 0.01$) so as not to violate the assumption

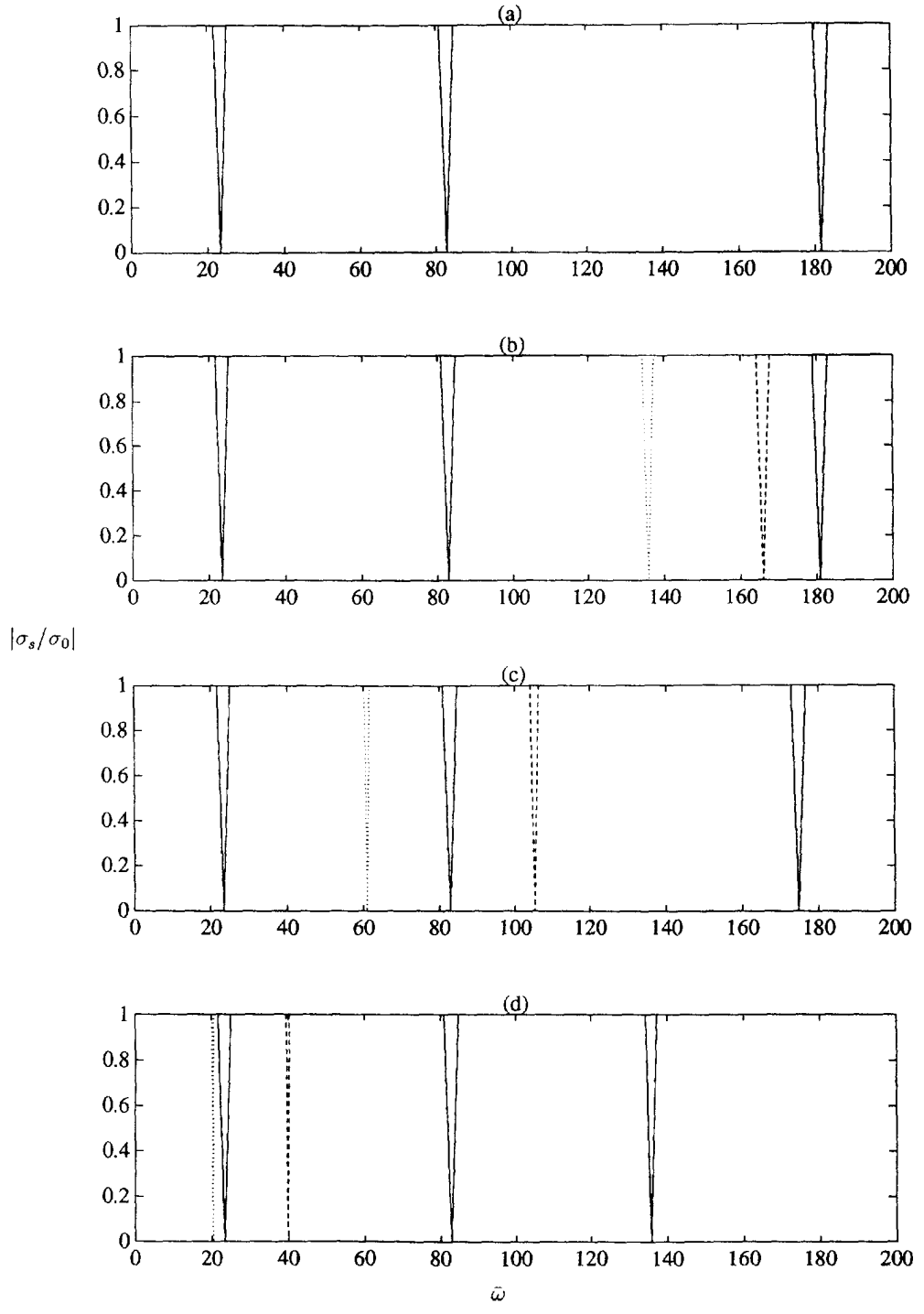

Fig. 4. The instability diagrams for an inextensible beam subjected to tensile pulsating axial loads. The initial shape is the third assumed mode. ———, $\bar{q}_{03} = 0.001$; - - - -, $\bar{q}_{03} = 0.005$; · · · · ·, $\bar{q}_{03} = 0.01$. (a) $\kappa = 0$, (b) $\kappa = 1$, (c) $\kappa = 10$, (d) $\kappa = 100$.

of small curvature. When the tip mass is large (for example, $\kappa = 100$), the shifting of the second unstable region may be large enough to make the frequency of perturbation smaller than the frequency of perturbation for the first unstable region with no tip mass. Once again, the remaining unstable regions remain relatively unaffected by variations in both the tip mass and the initial curvature. Similar conclusions can be drawn from the numerical results shown in Fig. 4 for the initial shape of the beam in the third assumed mode. The

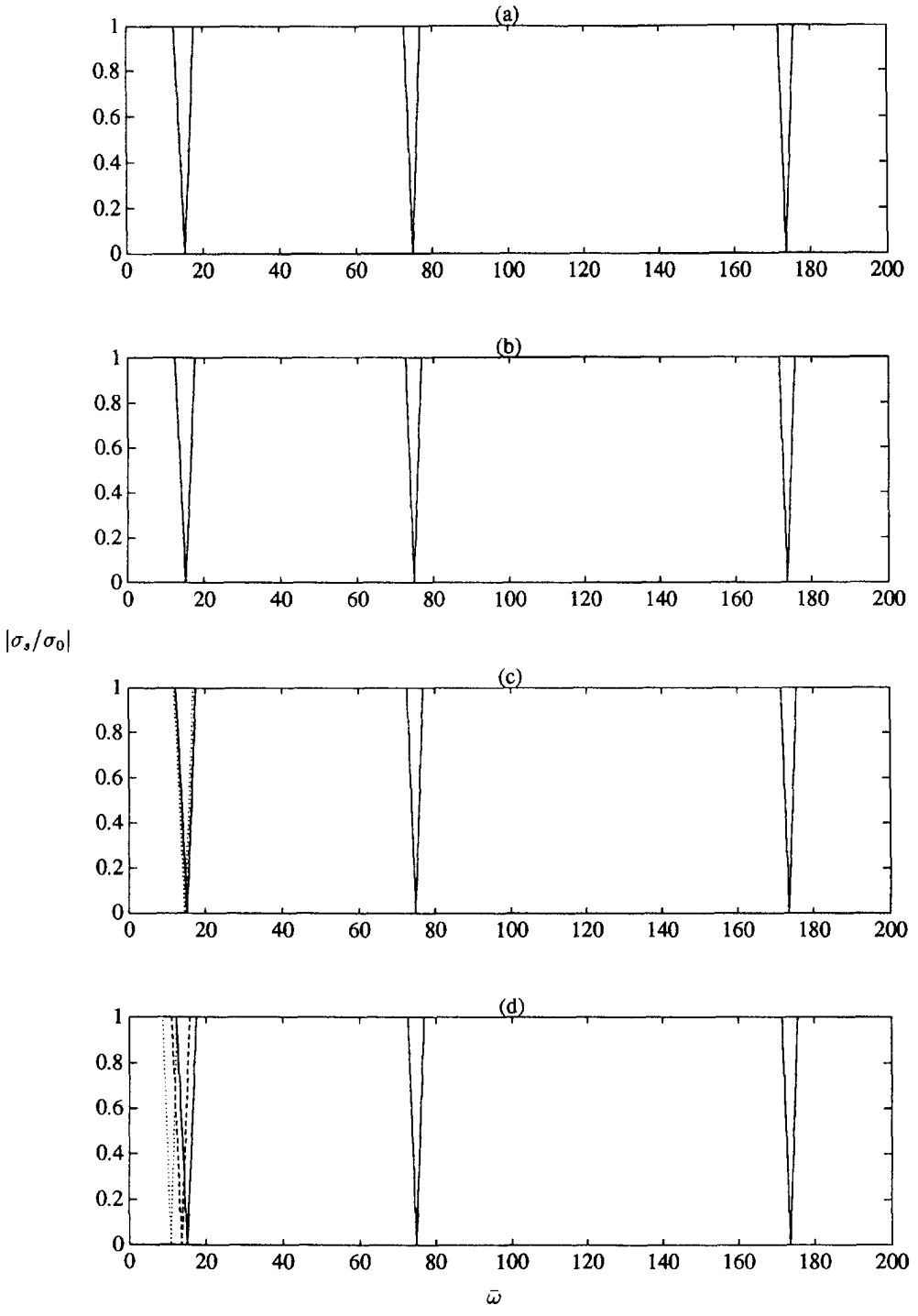

Fig. 5. The instability diagrams for an inextensible beam subjected to compressive pulsating axial loads. The initial shape is the first assumed mode. ———, $\bar{q}_{01} = 0.001$; - - - -, $\bar{q}_{01} = 0.005$; · · · · ·, $\bar{q}_{01} = 0.01$. (a) $\kappa = 0$, (b) $\kappa = 1$, (c) $\kappa = 10$, (d) $\kappa = 100$.

first two unstable regions, counted when there is no tip mass, remain unaffected while the third unstable region is shifted to the left with decreasing frequency of perturbation when the tip mass and the amplitude $\bar{q}_{03}$ are increased.

The effects of compressive axial pulsating loads on the instability diagrams are shown in Figs 5–7 for $\sigma_0 = -4$. The first critical Euler buckling load for a simply supported beam is $\sigma = \pi^2$. This value of $\sigma_0 = -4$ will ensure that the compressive axial loads are smaller

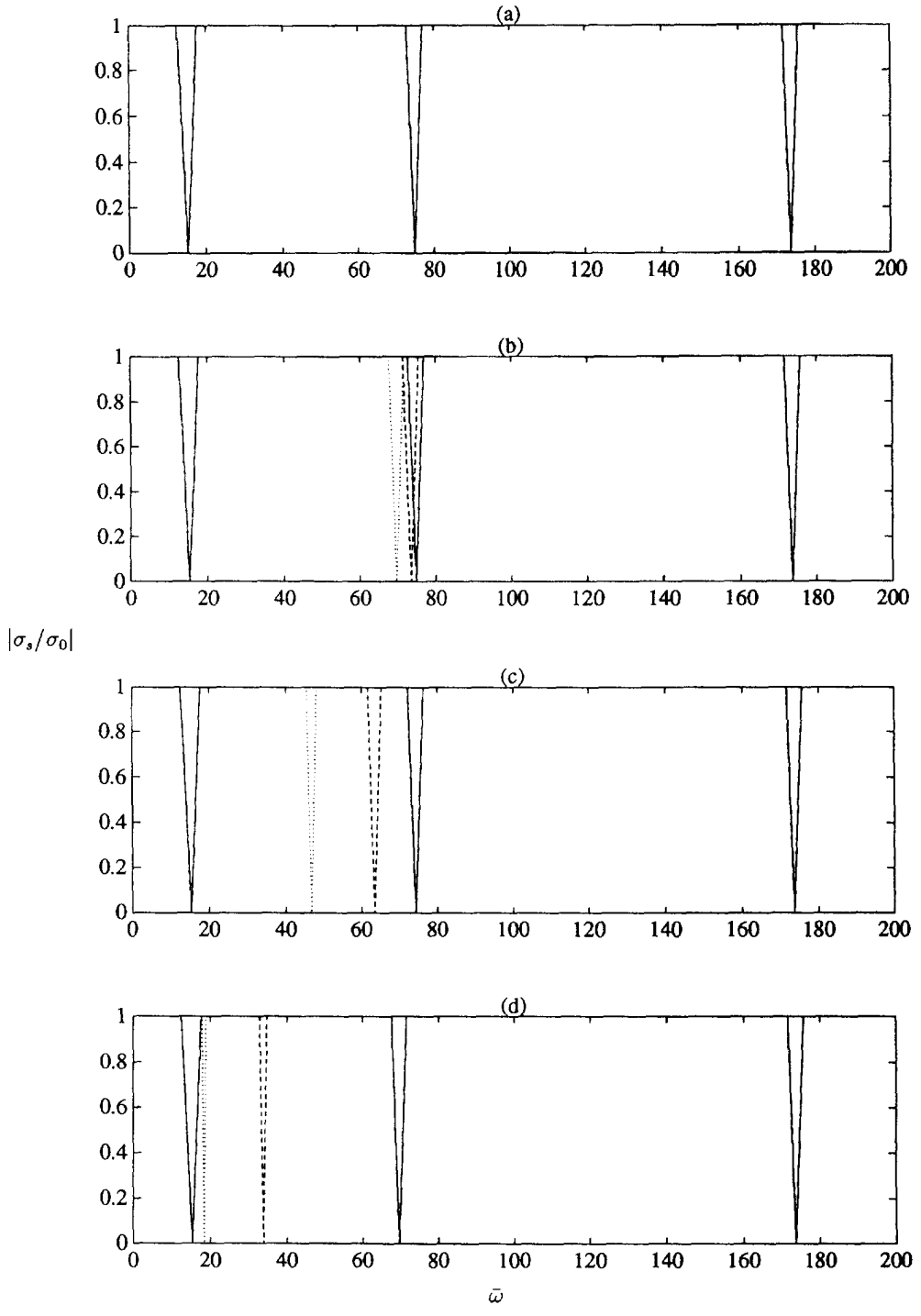

Fig. 6. The instability diagrams for an inextensible beam subjected to compressive pulsating axial loads. The initial shape is the second assumed mode. ———, $\bar{q}_{02} = 0.001$; - - - -, $\bar{q}_{02} = 0.005$; · · · · · $\bar{q}_{02} = 0.01$. (a) $\kappa = 0$, (b) $\kappa = 1$, (c) $\kappa = 10$, (d) $\kappa = 100$.

than the first critical buckling load at all times. This is also the reason as to why $\sigma_0 = 4$ for the numerical results presented in Figs 2–4. This is to allow for simple comparisons of the graphical results in Figs 2–4 with the present numerical results for compressive axial pulsating loads. As expected, it can be seen from Figs 5–7 that all the unstable regions are shifted to the left with smaller frequency of perturbation due to the compressive axial loads compared with the corresponding unstable regions shown in Figs 2–4 for a beam subjected

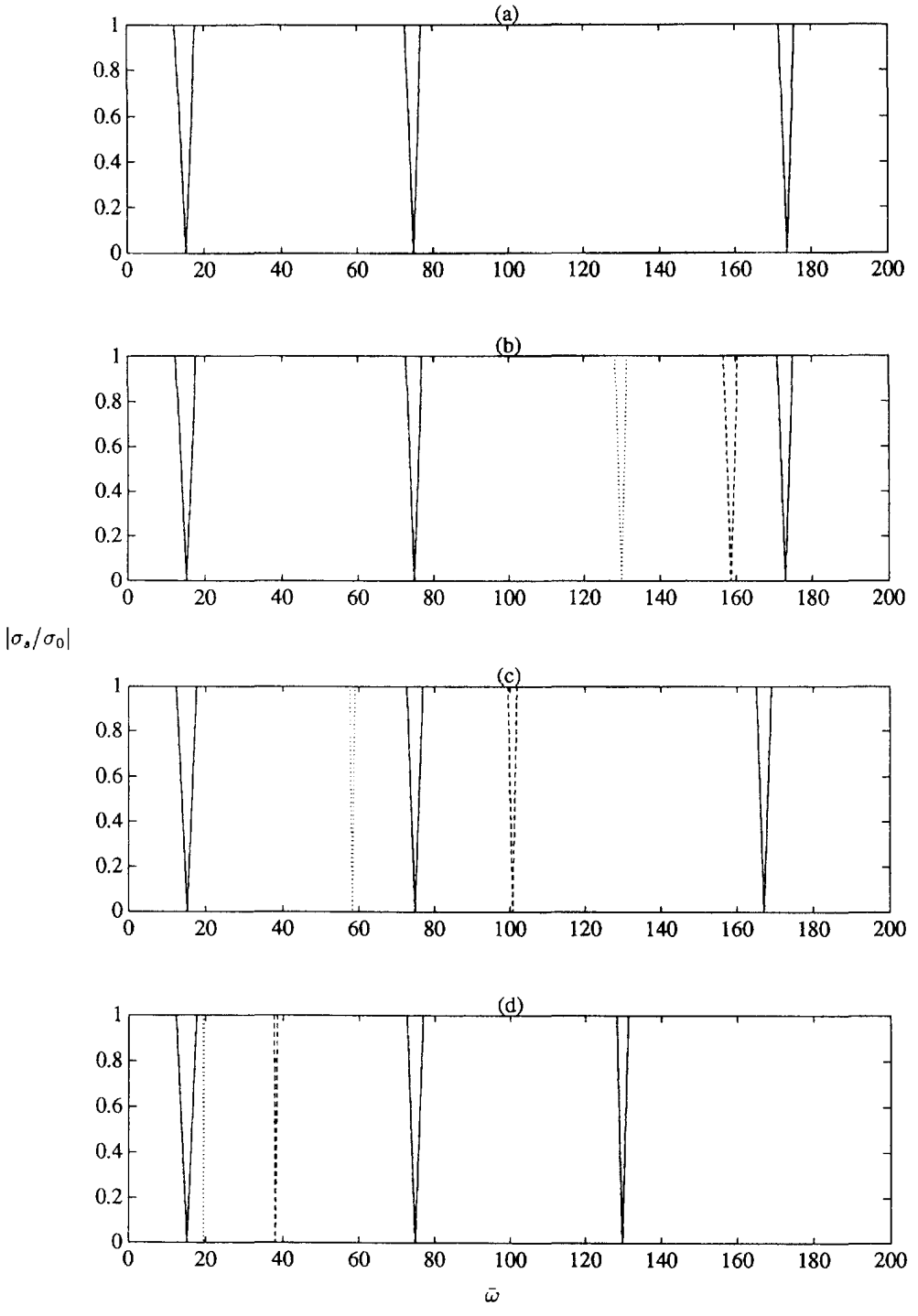

Fig. 7. The instability diagrams for an inextensible beam subjected to compressive pulsating axial loads. The initial shape is the third assumed mode. ———, $\bar{q}_{03} = 0.001$; - - - -, $\bar{q}_{03} = 0.005$; · · · · ·, $\bar{q}_{03} = 0.01$. (a) $\kappa = 0$, (b) $\kappa = 1$, (c) $\kappa = 10$, (d) $\kappa = 100$.

to tensile axial loads. Besides this finding, the same phenomenon of shifting of the unstable regions is observed with regards to variations in tip mass and the prescribed initial shape of the beam. If the initial prescribed shape of the beam is the pth assumed mode, the pth unstable region, counted for a beam with no tip mass, is shifted to the left with smaller frequency of perturbation when the tip mass is larger and the initial curvature of the beam is increased. The remaining unstable regions remain relatively unaffected.

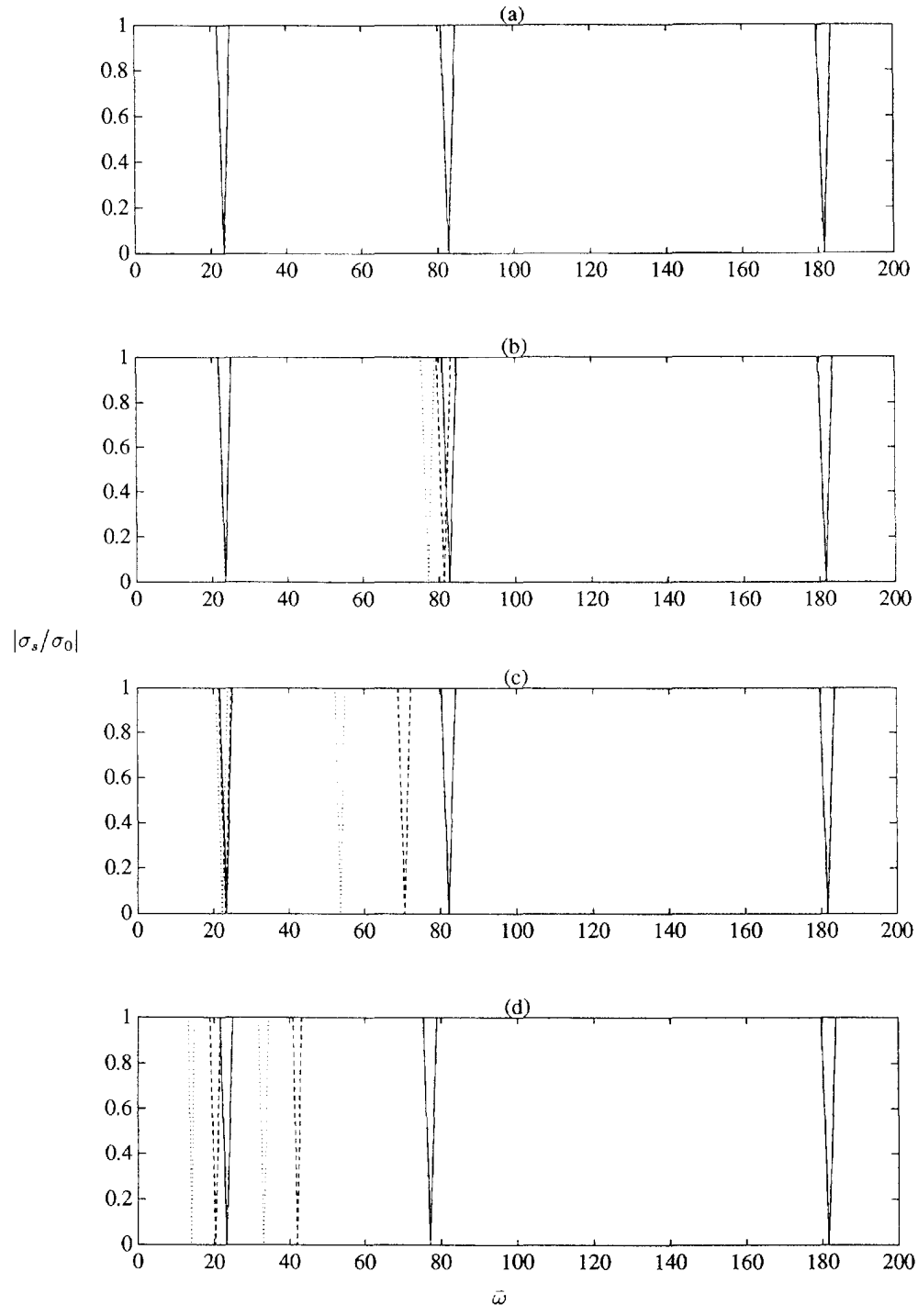

Fig. 8. The instability diagrams for an inextensible beam subjected to tensile pulsating axial loads. The initial shape is a combination of the first and the second assumed modes. ———, $\bar{q}_{01} = \bar{q}_{02} = 0.001$; - - - -, $\bar{q}_{01} = \bar{q}_{02} = 0.005$; · · · · ·, $\bar{q}_{01} = \bar{q}_{02} = 0.01$. (a) $\kappa = 0$, (b) $\kappa = 1$, (c) $\kappa = 10$, (d) $\kappa = 100$.

The instability diagrams for a beam subjected to tensile axial pulsating loads ($\sigma_0 = 4$) with the initial shape described by a combination of the first and the second assumed modes are shown in Fig. 8. It can be seen that both the first and the second unstable regions are affected by the changes in the amplitude of the prescribed initial shape, especially for a large lumped mass. However, if comparisons are made between Fig. 8(d) with that of Fig.

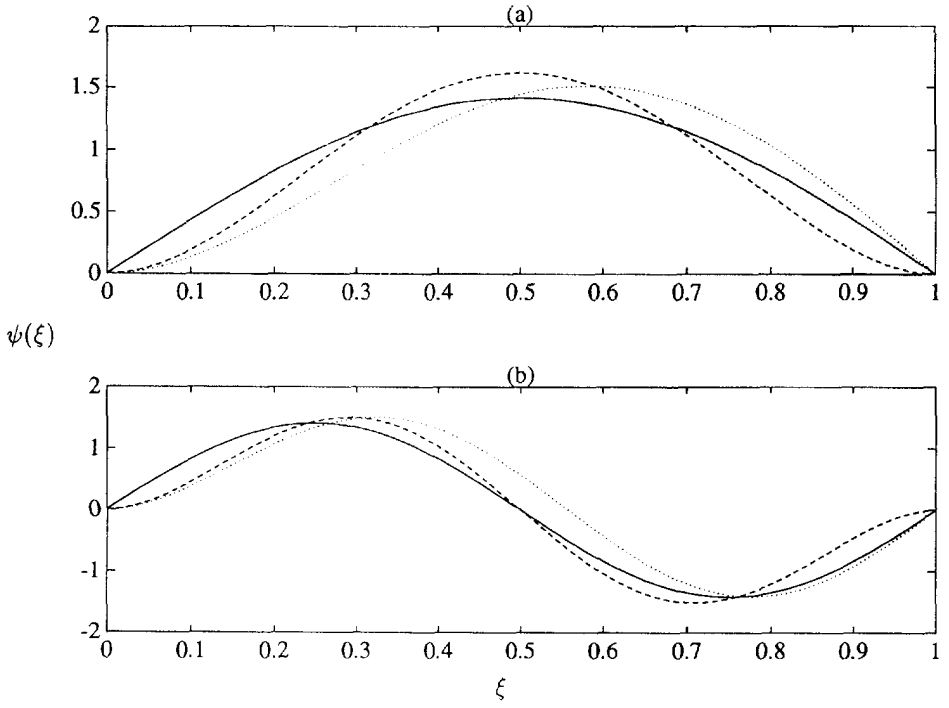

Fig. 9. The prescribed initial shape of the beam. ———, Simply supported–simply supported mode shape; - - - -, clamped–clamped mode shape; · · · · ·, clamped–simply supported mode shape. (a) The first mode, (b) the second mode.

2(d) and Fig. 3(d), it can be seen that the locations of the unstable regions are quite different. The main reason is that for such a beam with the initial shape given by a combination of the assumed modes, the $\bar{\mathbf{S}}$ matrix is no longer a diagonal matrix as $\bar{\mathbf{q}}_0\bar{\mathbf{q}}_0^T$ within the $\bar{\mathbf{S}}$ matrix is not a diagonal matrix, although $\bar{\mathbf{Q}}$ remains a diagonal matrix due to the orthogonality of the assumed functions.

The case of a beam with the initial shape $\bar{y}_0$ different from any of the assumed modes for $\bar{w}$ is examined with the initial shape described respectively by the normalized first and second modes for the free vibration of a clamped–clamped beam and a clamped–simply supported beam. These various cases of prescribed initial shapes of the beam are plotted with the first and the second assumed mode shapes for $\bar{w}$ in Fig. 9. The instability diagrams for a beam with a large lumped mass ($\kappa = 100$) subjected to tensile axial pulsating loads ($\sigma_0 = 4$) are shown in Fig. 10. It can be seen from Fig. 10(a,b) that the second unstable regions are affected more significantly by the variation in the amplitude of the initial shape when the initial shape is in the form of the first or second mode of a clamped–clamped beam. However, the first and the third unstable regions are relatively unaffected by variation in the amplitude of the initial shape. On the other hand, when the initial shape is in the form of the first or the second mode for the free vibration of a clamped–simply supported beam [Fig. 10(c,d)], all of the first three unstable regions are affected by variation in the amplitude of the initial shape. Therefore, it can be concluded in general that if the initial shape is not in the form of combinations of any of the assumed modes for $\bar{w}$, all the unstable regions are likely to be affected by variation in the amplitude of the initial shape. Numerical results for other forms of initial shapes can also be easily computed using the present formulation.

CONCLUSION

The linearized equation of motion in matrix form of an inextensible Euler–Bernoulli beam with initial curvature subjected to pulsating axial load has been formulated based on Lagrangian approach and the assumed mode method. A tip mass is assumed to be attached

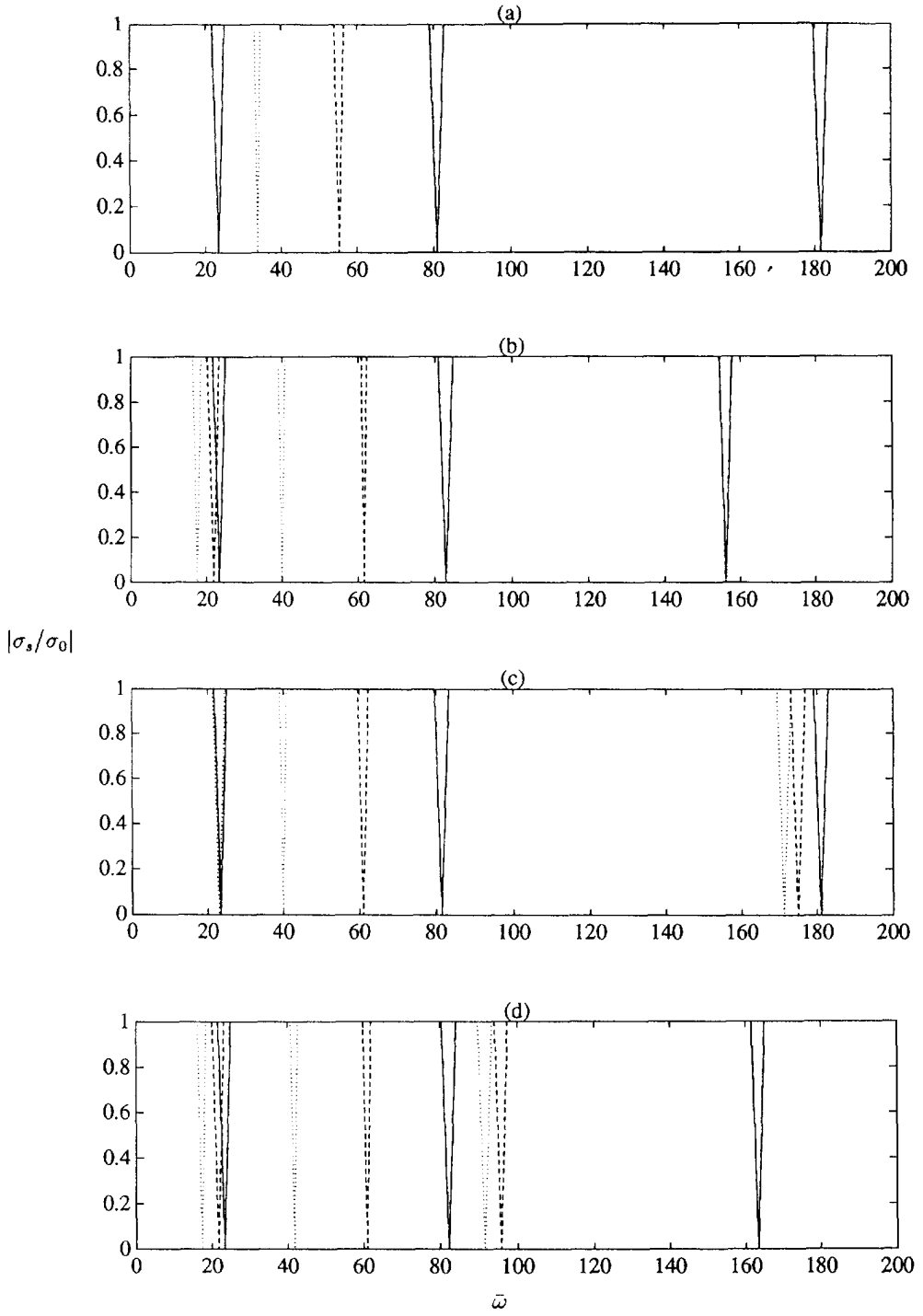

Fig. 10. The instability diagrams for an inextensible beam subjected to tensile pulsating axial loads with $\kappa = 100$. ———, $\bar{q}_{01} = 0.001$; - - - -, $\bar{q}_{01} = 0.005$; · · · · ·, $\bar{q}_{01} = 0.01$. The initial shape $\bar{\psi}_1$ is (a) the first mode of a clamped–clamped beam, (b) the second mode of a clamped–clamped beam, (c) the first mode of a clamped–simply supported beam, (d) the second mode of a clamped–simply supported beam.

to the end of the beam. The effects of initial curvature are found to be contained in the kinetic energy of the tip mass as well as the work done by the axial loads. The equation of motion is then converted to the standard form of an eigenvalue problem for computing the principal instability regions using Bolotin's method. The prescribed initial shape of the beam is found to have no effect on the stability of the beam when there is no tip mass.

When there is a tip mass, the effect of the initial curvature of the beam becomes more pronounced with increased curvature of the beam. Moreover, the initial prescribed shape of the beam may drastically affect the instability regions of the beam with a tip mass. If the initial prescribed shape of the beam is the pth assumed mode, the pth unstable region (counted for a beam with no tip mass) is shifted to the left with smaller frequency of perturbation when the tip mass is larger and the initial curvature of the beam is increased. The remaining unstable regions remain relatively unaffected. As expected, an increase in the average compressive axial loads tends to shift the unstable regions to the left with smaller frequency of perturbation.

REFERENCES

Bolotin, V. V. (1964). *The Dynamic Stability of Elastic Systems*. Holden-Day, San Francisco.

Carlson, R. L., Lo, H. C. T. and Briley, R. P. (1980). On the parametric excitation of a tensioned bar with initial curvature. *Int. J. Mech. Sci.* **22,** 59–65.

Dickinson, S. M. (1980). The lateral vibration of slightly bent slender beams subjected to prescribed axial end displacement. *J. Sound Vibration* **68,** 507–514.

Ilanko, S. (1990). The vibration behavior of initially imperfect simply supported beams subjected to axial loading. *J. Sound Vibration* **142,** 355–359.

Johnson, E. R. (1982). Load–frequency relations for a clamped shallow circular arch. *AIAA J.* **20,** 1763–1765.

Kim, C. S. and Dickinson, S. M. (1986). The flexural vibration of slightly curved slender beams subjected to axial end displacement. *J. Sound Vibration* **104,** 170–175.

Masurekar, V. and Gupta, K. N. (1987). Stability analysis of four bar mechanism (Part I) with the assumption that damping is absent. *Mech. Machine Theory* **23,** 367–375.

Plaut, R. H. and Johnson, E. R. (1981). The effect of initial thrust and elastic foundation on the vibration frequencies of a shallow arch. *J. Sound Vibration* **78,** 565–571.

Saito, H. and Koizumi, N. (1982). Parametric vibrations of a horizontal beam with a concentrated mass at one end. *Int. J. Mech. Sci.* **24,** 755–761.

Takahashi, K. (1981). An approach to investigate the instability of the multiple-degree-of-freedom parametric dynamic systems. *J. Sound Vibration* **78,** 519–529.

Yamaki, N. and Mori, A. (1980). Non-linear vibrations of a clamped beam with initial deflection and initial axial displacement, Part I : theory. *J. Sound Vibration* **71,** 333–346.

Yamaki, N., Otomo, K. and Mori, A. (1980). Non-linear vibrations of a clamped beam with initial deflection and initial axial displacement, Part II : experiment. *J. Sound Vibration* **71,** 347–360.